



*Research article*

## **Lightweight design method and application of MEWP bracket based on multi-level optimization**

**Wen Li<sup>1,2</sup>, Jian Wang<sup>3</sup>, Zhanpeng Du<sup>3,\*</sup>, Hongfeng Ma<sup>2</sup>, Lijie Zhang<sup>1</sup> and Libin Duan<sup>3</sup>**

<sup>1</sup> Hebei Provincial Key Laboratory of Heavy Machinery Fluid Power Transmission and Control, Yanshan University, Qinhuangdao 066004, China

<sup>2</sup> Jiangsu XCMG State Key Laboratory Technology Co., Ltd., Xuzhou 221000, China

<sup>3</sup> Institute of Lightweight and Safety of New Energy Vehicle, School of Automotive and Traffic Engineering, Jiangsu University, Zhenjiang 212013, China

\* **Correspondence:** Email: [dzp1014@163.com](mailto:dzp1014@163.com); Tel: +8618775280696.

**Abstract:** Mobile elevating work platform (MEWP) is a large-scale engineering machinery equipment that transports workers and tools to the designated height for operation. As the key supporting component of MEWP, the bracket simultaneously needs to meet the performances of high stiffness and strength. Furthermore, the mechanical performance of the bracket can be significantly influenced by its cross-sectional shape. However, the optimal cross-sectional shape of bracket is not easily to obtain owing to the lacking of lightweight design method. Thus, a lightweight design method of MEWP bracket based on multi-level optimization is proposed in this paper. Firstly, the multi-case topology optimization model of MEWP bracket is constructed by using the compromise programming method, and the optimal section configuration of MEWP bracket is obtained based on Solid Isotropic Material with Penalization (SIMP). Secondly, the parameterization of the cross-sectional shape of bracket is realized using the mesh deformation technology, and the multi-case optimization mathematical model of the MEWP bracket is established. Then, the cross-sectional shape and gauge of the bracket are optimized using multi-level optimization method. The optimized results show that weight reduction mass is 11.66 kg and the ratio is 52.4% under the premise that the stiffness of the bracket does not decrease. Furthermore, the weight of MEWP bracket optimized by the multi-level optimization method reduced by 1.27 kg compared with single gauge optimization method. Finally, a physical prototype is developed according to the optimization results.

**Keywords:** MEWP; bracket; lightweight design; multi-level optimization method

## 1. Introduction

Aerial work platform has the advantages of flexible movement, convenient height adjustment and improving the efficiency of operation. Four typical aerial work platforms are shown in Figure 1. The key premise of aerial work platform is safety and stability. In practical engineering, accidents easily occur due to the insufficient carrying capacity of bracket during operation. Thus, it is necessary to improve the stiffness, strength, and reduce the overall weight when designing the aerial work platform.



(a) Straight arm type (b) Curved arm type (c) Scissor type (d) Mast column type

**Figure 1.** Physical drawing of typical aerial work platform.

The operation sensitivity of aerial work platform is reduced due to large weight, which affects its work efficiency. Thus, the lightweight design of aerial work platform is greatly significant for improving the working performance. At present, the structural lightweight design of aerial work platform has been proved in the boom part. Zhang and Liu [1] took the boom mass as the object, and the yield strength and stiffness of the material were set as the constraint. Then, the Pareto front of each boom section size are obtained based on NSGA-II algorithm. The results show that the weight of the optimized arm is reduced by 13.3% compared with the original design. As the key supporting component of the working platform, there are few relevant research reports on the structural lightweight design of bracket. Moreover, the optimal cross-sectional shape of bracket is not easily to obtain owing to the lacking of lightweight design method, which increases the difficulty of realizing the structural lightweight. In order to find the best distribution of materials and improve design efficiency, multi-objective structural optimization under multi-cases has received extensive attentions in recent years. It is composed of topology optimization, size optimization and morphology optimization. Gui et al. [2] developed a multi-objective and multi-case reliability optimization design to improve the crashworthiness of TRB and realize lightweight at the same time. The radial basis function element model was used to construct the response of objectives and constraints. The NSGA-II combined with Monte Carlo Simulation (MCS) was used to find the reliability solution. The optimization results show that the proposed method improves the reliability of Pareto solution and increases the robustness under MLC. Duan et al. [3] carried out multi-objective reliability optimization

design for automobile front longitudinal beam (FLB). The results show the variable-rolled-blank and variable-cross-sectional-shape FLB (VRB-VCS FLB) have better lightweight and crashworthiness under constraints. The results show that when compared with uniform-thickness FLB, the crashworthiness and reliability of VRB-VCS FLB are significantly improved. Qiu et al. [4] carried out topology optimization under the combined axial and transverse load of multi cell hexagonal tube. The improved particle swarm optimization algorithm was used to improve the success rate of global optimization. The results show that the optimized material is placed outward to increase the moment of inertia and resist the overall deformation. Ahmad et al. [5] proposed the application of topology optimization and response surface method to the lightweight design of automatic vehicle crank arm. They carried out topology optimization under the creation of multiple loads on the crank. The shape is optimized to minimize the stress concentration at the corner by response surface method. The results show that the two optimization methods can reduce the mass of the crank arm and reduce the maximum stress of the crank arm to 20%. Du et al. [6] took the minimum flexibility of the overall structure as the object and used the weight compromise programming method to construct the mathematical optimization model of multi-case topology optimization. Then, they obtained the optimal topology of the tower belt working platform and reconstructed the geometric model. The results show that the optimized structure reduces its own weight and stress. In addition, the stiffness is improved. Wang et al. [7] developed several static and modal analysis on the engine accessory support. Then, structural weight minimization model with displacement and frequency constraints was constructed to obtain an optimal topology under multiple load cases. The results show that this method reduces the weight of the support and improves the stiffness of structure. Zhu et al. [8] proposed an effective numerical method to realize the multi-case optimization design of heat conduction problems. The level set model is used to implicitly represent the geometric boundary of heat conducting materials. In addition, the topological derivative is introduced to generate a new topology in a new field of design. In the analysis, the shape is taken as the design variable and the quadratic temperature gradient function is taken as the objective function. The function obeys the steady-state heat conduction equation of state and volume constraints. Numerical examples show that the proposed method is effective and robust in topology optimization of heat conduction problems.

It can be concluded that the structural optimization design has been applied in many disciplines and fields, and the effectiveness of its method is proved. Thus, this paper applies the structural topology and gauge optimization method to the lightweight design of MEWP platform bracket structure to reduce the material consumption.

In the process of structural optimization design of aerial work platform, the optimization design is carried out according to the changes of topological configuration, cross-sectional shape and gauge at different development stages. However, the design engineers mainly rely on their own experience and analyze the past product database when making decisions on the cross-section shape of the high-altitude platform frame. In addition, a large number of design variables lead to unclear direction and great limitations. Thus, Duan et al. [9] proposed a lightweight design strategy of BIW integrating implicit parameterization technology, global sensitivity analysis (GSA) and Pareto set pursuing (PSP) algorithm. The results show that the optimized BIW structure is significantly improved compared with the baseline model. In terms of mesh parameterization and deformation technology, Mi et al. [10] proposed a parameterized direct manipulation free deformation method to realize the process of geometric parameterization and mesh deformation. The elliptical airfoil is optimized to improve its aerodynamic performance. Zhang and Feng [11] established a thin-walled structure through the

method of mesh parameterization and completed the stiffness layout optimization of complex surfaces. Numerical examples show the advantages and effectiveness of this method. Zhang et al. [12] used response surface method and mesh deformation technology to automatically optimize the feeding chamber of extrusion die. The velocity distribution in the cross section of the optimized profile tends to be more uniform. Wang et al. [13] established a parametric model of the subframe with 12 geometric parameters as the design variables, and take the weight, maximum von Mises stress and first-order natural frequency as the objective function based on the mesh deformation technology. The improved NSGA-II was used to optimize the subframe and determine a set of Pareto optimal solutions. Nazemian and Ghadimi [14] used the mesh deformation tool to change the geometry and took the position of the mesh deformation control point as the design variable used in the optimization process. The results show that the total resistance of trimaran decreases by 6.67% in a limited number of iterations which proves the ability of mesh deformation with complex geometric methods.

With the improvement of computer performance and optimization design requirements, scholars are no longer limited to the weight as the objective function. The reliability, manufacturing difficulty and economy of the structure are added to the objective function. Thus, multi-level optimization technology is introduced to carry out multi-disciplinary and multi-objective structural optimization design. The original optimization problem is decomposed into a series of independent secondary problems and then solved. The more complex the structure is, the easier it can reflect the convenience brought by the multi-level optimization technology, especially for large engineering structures. Hou et al. [15] proposed a conceptual design tool based on the global body skeleton optimization algorithm. The conceptual design tool applies the multi-level optimization algorithm to optimize the body performance. It is shown that the overall stiffness and vibration characteristics of the body are optimized when reducing the body mass. Gandikota et al. [16] proposed a decomposition formula and solution method for multidisciplinary vehicle design optimization under the design criteria of crashworthiness, occupant safety, mass and vibration. The multi-level optimization problem is composed of the minimization of damage criteria at the system level and the minimization of independent mass at the subsystem level. The final mass is reduced by 8.7 kg. Liu et al. [17] used multi-level optimization strategy to determine a propeller with high efficiency and light weight. The NSGA-II is applied to maximize the propeller efficiency and minimize the propeller weight. The results show that the optimized propeller has light weight and good aerodynamic performance.

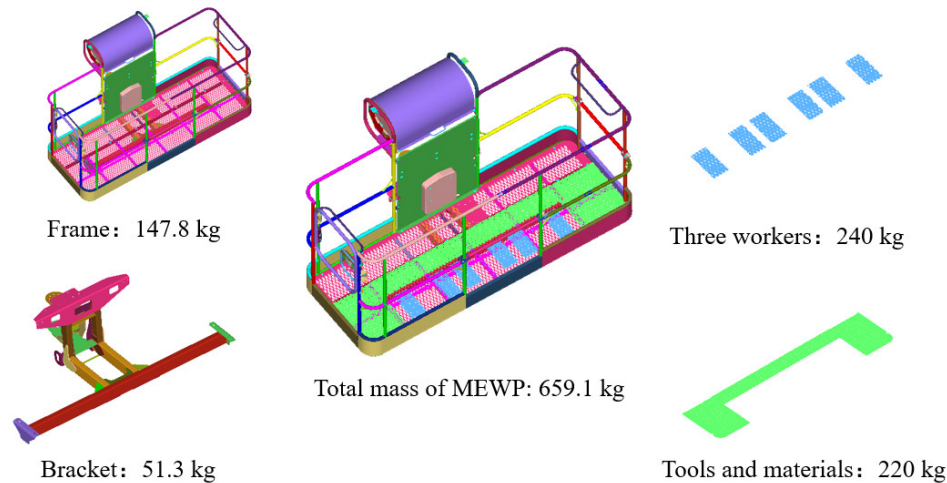
It can be seen that multi-level optimization design is widely used in automotive and other fields. However, the multi-level optimization design of MEWP bracket has not formed a systematic method system. Thus, in Section 2, this paper takes MEWP as the research object and analyzes the displacement of locking tab and two sensors under five typical stiffness conditions. In Section 3, the lightweight design of bracket is carried out under the condition of meeting the evaluation index and performance requirements based on the multi-level optimization method. In order to prove the effectiveness of multi-level optimization method, the comparison of optimization effects under two means of optimization is carried out. Finally, a summary of the findings is concluded in Section 4.

## **2. Multi-case topology optimization of MEWP bracket structure**

### *2.1. Overview of initial design*

The three-dimensional modeling is carried out through HyperMesh according to the structural

dimensions of the MEWP. Since the small structures such as fillets have little effect on the analysis of the finite element surface model structure, moreover, in order to reduce the calculation amount of finite element analysis, the fillets and threaded holes between various sections are removed from the established model. The welding joint is treated according to the constraints of RIGIDS and RBE2. The bolt is simulated by rigid element, the frame and the bracket are weld by shell element and entity element, respectively. The personnel weight shall be evenly distributed according to the contact surface of both feet, and the tools and materials shall be evenly distributed as well. The structure of MEWP working platform is shown in Figure 2.



**Figure 2.** Finite element model of MEWP and bracket.

This paper takes the MEWP bracket as the analysis object and carries out static analysis in Optistruct solver. The material parameters of bracket are shown in Table 1.

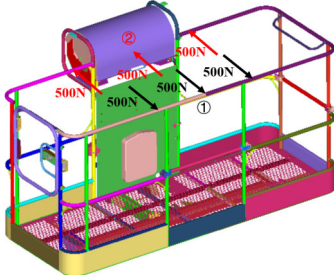
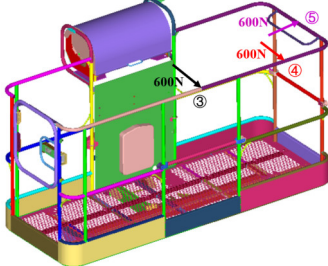
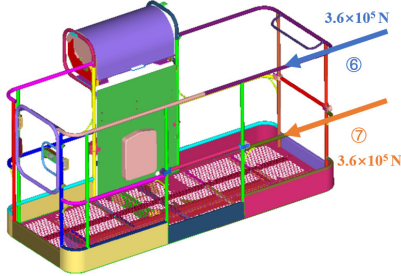
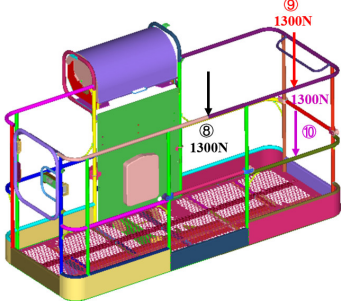
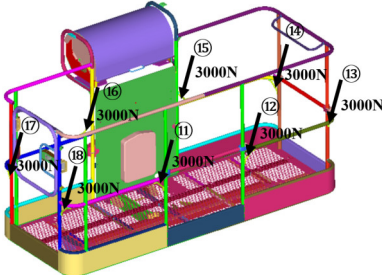
**Table 1** Physical properties and parameters of bracket.

Rectangular tube	Material	Gauge (mm)	Mass (kg)	Young's modulus (GPa)	Yield stress (MPa)	Density (g/cm <sup>3</sup> )	Poisson's ratio
1	Q345	3	11.240	210	345	7.83	0.3
2	Q345	3	6.475	210	345	7.83	0.3
3	Q345	3	4.525	210	345	7.83	0.3

## 2.2. MEWP stiffness analysis and evaluation index

The overall mass of MEWP is 659.1 kg and the mass of bracket is 22.24 kg. As a key carrying component, the structure and mass of bracket affect the sensitivity and operational stability of the MEWP. Thus, MEWP is applied by corresponding loads and constraints according to the requirements of national regulations and enterprise standards. Then, stiffness analysis of the MEWP is carried out, and the deformation capacity of the locking tab and two sensors are evaluated. The information of five optimized working conditions and corresponding loading force established is shown in Table 2.

**Table 2.** Five optimized working conditions.

Working condition	Analysis items	Finite element model
1	Deformation resistance of guardrail (Applying a concentrated load of 500 N at an interval of 0.5 m at the most unfavorable position and direction of the guardrail)	
2	Platform stiffness (Applying a force of 600 N in any direction at the edge of MEWP)	
3	Guardrail stiffness (Applying 360 N load on the top railing and middle cross bar of the working platform in the horizontal direction)	
4	Top of guardrail, handrail and middle cross bar (Applying a concentrated load of 1300 N in the vertical direction to the top railing or middle cross bar)	
5	Safety belt nodes (Applying a concentrated load of 3000 N at the safety belt node of MEWP)	

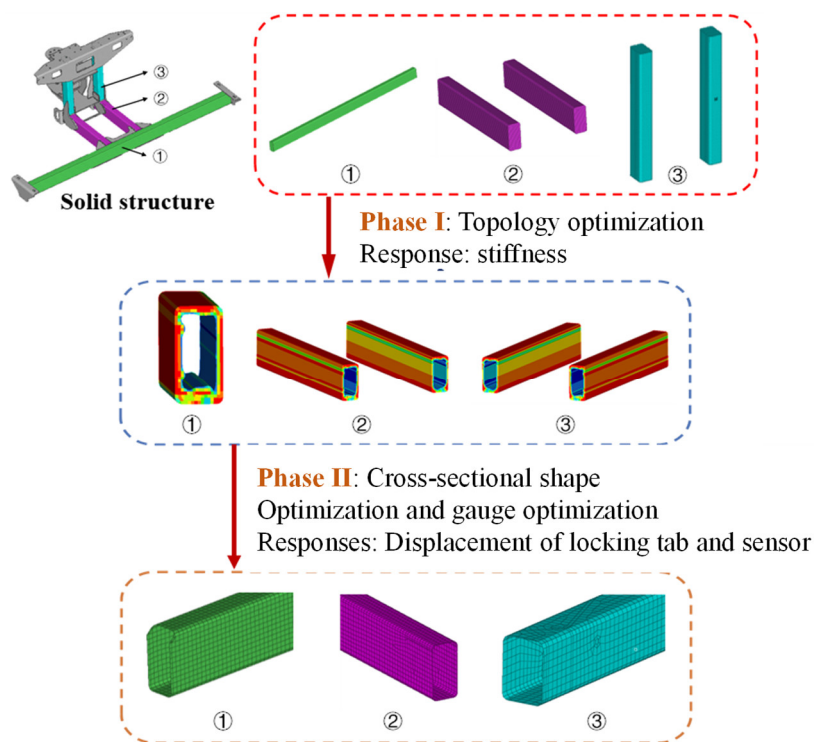
In order to simplify the model and improve the accuracy and efficiency of calculation, the static general analysis step is used in the simulation process. The upper and lower inner rings of the bracket sensor are rigidly connected, and the central reference point is set to restrict all the degrees of freedom of the central point. The welds of the bracket arm are simulated by solid elements. The structural



stiffness of MEWP working platform meets the requirements of national regulations and enterprise standards obtained through HyperWorks/Optistruct analysis under the above five stiffness conditions.

### 3. Multi-level optimization design of MEWP bracket structure

The multi-level optimization method is introduced to solve the optimization problem of complex design variable coupling for the conceptual design of MEWP bracket structure. The design flow chart is shown in Figure 3. Firstly, the multi-case topology optimization model of MEWP bracket is constructed based on the compromise programming method. On the premise of meeting five conditions, the optimal section configuration of MEWP bracket is determined by SIMP topology optimization theory. Secondly, the parameterization of the section shape of the bracket structure is realized based on the grid deformation technology. Moreover, the multi-case optimization mathematical model of the MEWP bracket is established, and the section shape and gauge of the MEWP bracket are optimized by using the Latin square sampling method and the Global Response Surface Method.

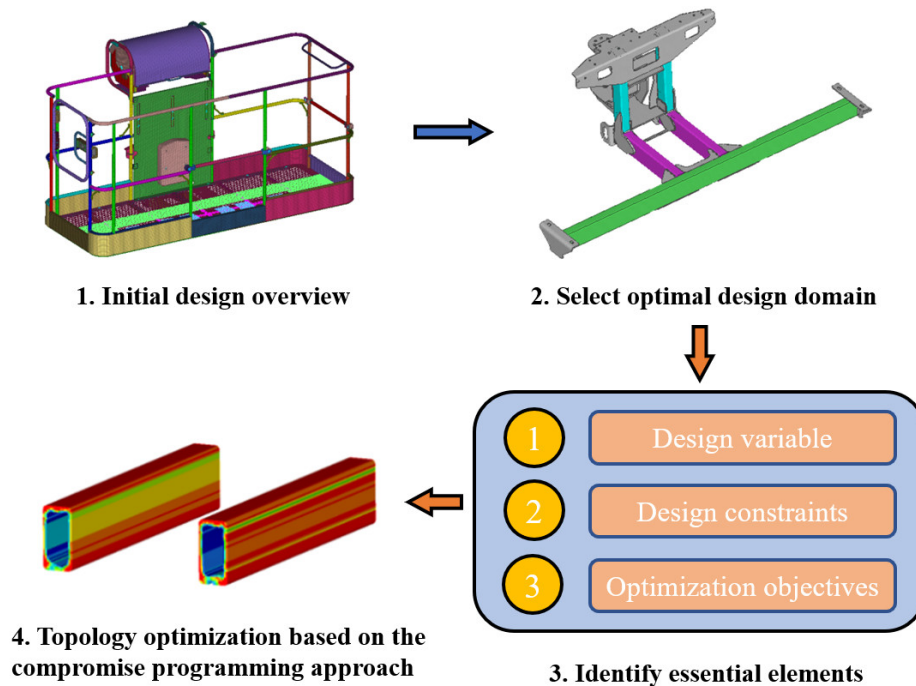


**Figure 3.** Multi-level optimization design process of MEWP bracket.

#### 3.1. Phase I: Multi-case topology optimization

In order to obtain the preliminary section topology configuration of MEWP bracket in the conceptual design stage, this paper constructs the multi-case topology optimization model of MEWP bracket based on the compromise programming method. The specific process is presented in Figure 4. Firstly, the displacement of locking tab and two sensors of MEWP bracket under five working conditions is evaluated. Then, the design domain and the basic three elements of topology optimization are determined, and the optimal section configuration of MEWP bracket is obtained by SIMP method.

Finally, the compromise programming model is introduced based on SIMP method to solve the optimal energy transfer model under each target condition.



**Figure 4.** Multi-case topology optimization process of MEWP bracket.

The choice of material units in the design area is analyzed according to optimal material distribution proposed by Bendsøe and Kikuchi [18]. By using the material effectiveness characteristic function, the physical model can be transformed into a mathematical model for numerical calculation of optimization problems.

$$\chi(\rho) = \begin{cases} 1, & \rho \in \Omega_{mat} \\ 0, & \rho \in \Omega_{void} \end{cases} \quad (1)$$

where  $\rho$  indicates the material density;  $\Omega_{mat}$  represents the part where the material exists in the structure;  $\Omega_{void}$  represents the part where the material does not exist in the structure.

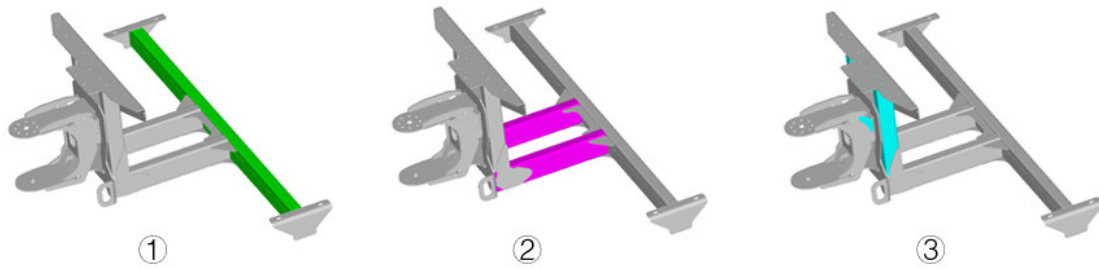
The SIMP function model based on the relationship between the relative element density  $x_e$  and Young's modulus  $E_0$  is:

$$E_e = E_{min} + x_e^p (E_0 - E_{min}), \quad x_e \in [0, 1] \quad (2)$$

where  $E_{min}$  is a value close to 0;  $p$  is the penalty factor. When the penalty factor is larger, the function value of simp is closer to 0 and 1, and the gray units are fewer.

MEWP bracket design domain is defined, as shown in Figure 5.





**Figure 5.** Topology optimization design domain.

This paper takes the element density  $x_e$  of bracket as the design variable and takes the minimum compliance  $C$  as the objective function. In addition, the volume fraction constraint and extrusion constraint with the upper limit of 30% is set, and the model of topology optimization problem based on SIMP method is obtained as follows:

$$\begin{aligned}
 \text{Find:} \quad & x_e = \{x_1 \ x_2 \ \dots x_N\}^T \in \Omega \\
 \text{Minimize:} \quad & C(x_e) = F^T U = \sum_{e=1}^N (E_{\min} + x_e^p (E_0 - E_{\min})) u_e^T k_0 u_e \\
 \text{Subject:} \quad & V^* \leq 0.3V \\
 & F = KU \\
 & 0 < x_{\min} \leq x_e \leq 1 (e = 1, 2, 3, \dots, n)
 \end{aligned} \tag{3}$$

where  $V^*$  represents the optimized volume;  $V$  is the initial volume;  $F$  is the load vector;  $K$  is the stiffness matrix;  $U$  is the displacement column vector;  $x_{\min}$  generally takes a value close to 0, such as 0.0001.

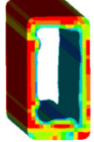
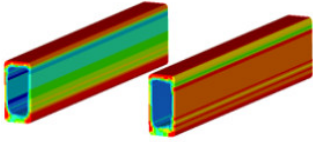
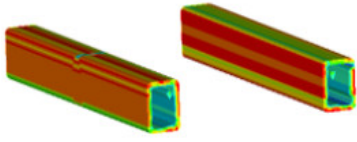
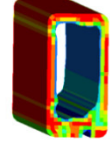
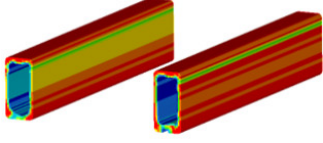
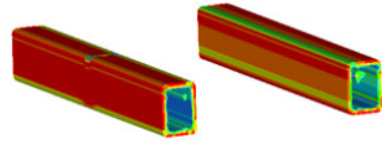

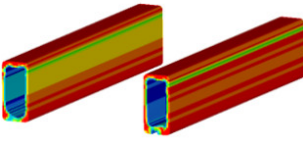
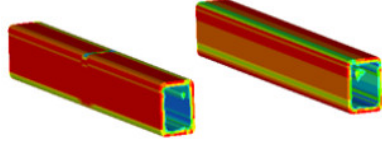
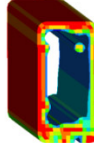
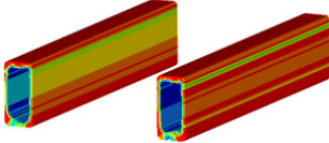
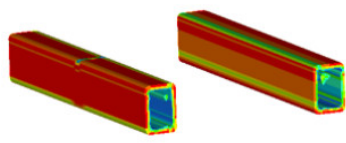
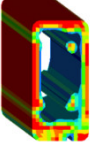
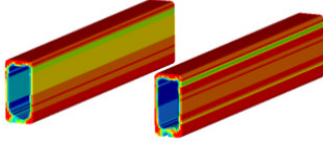
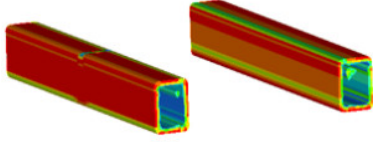
The topology optimization results of bracket under different working conditions are obtained by substituting the model into the solution as shown in Table 3.

In order to transform the multi-case function into a single objective function, an objective function is established which includes the best force transfer path of the structure under each condition. Thus, this paper introduces the normalized compliance objective function based on the compromise programming method by considering the topology optimization objective function of multi-case structure. The specific form is as follows:

$$\begin{aligned}
 \text{Find:} \quad & x_e = \{x_1, x_2, \dots, x_N\}^T \in \Omega \\
 \text{Minimize:} \quad & F(X) = \sum_{k=1}^5 \left( \omega_k \frac{C_k(\rho) - C_{k\min}}{C_{k\max} - C_{k\min}} \right), \quad k = 1 \sim 5 \\
 \text{Subject:} \quad & V^* \leq 0.3V \\
 & 0 < x_{\min} \leq x_e \leq 1 (e = 1, 2, \dots, N)
 \end{aligned} \tag{4}$$


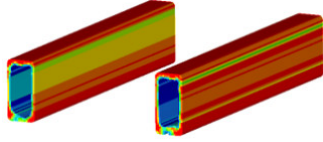
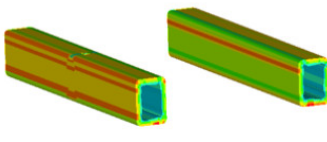
where  $\omega_k$  indicates the weight coefficient of the  $k$ -th working condition;  $C_k(\rho)$  is the structural compliance of the  $k$ -th working condition;  $C_{k\min}$ ,  $C_{k\max}$  is the minimum and maximum compliance after the optimization of the  $k$ -th single working condition, respectively.

**Table 3.** Topology optimization results of bracket under different working conditions.

Working conditions	Rectangular tube-1	Rectangular tube-2	Rectangular tube-3
1			
2			
3			
4			
5			

Since the difference of the order of magnitude between the five working condition loads applied to the structure is small, the working condition weight coefficient is set to 0.2. The optimized configuration of structural topology is obtained as shown in Table 4.

**Table 4.** Multi-case topology optimization results based on compromise programming model.

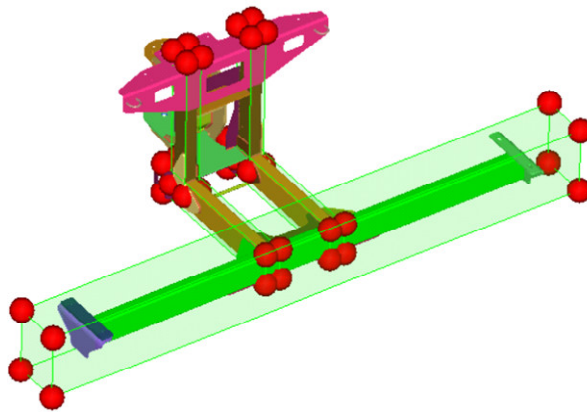
\	Rectangular tube-1	Rectangular tube-2	Rectangular tube-3
Multi-case topology results			
Height of cross section (mm)	97	97	67
Width of cross section (mm)	47	47	47
Length of rectangular tube (mm)	1740	498.5	449
Initial gauge (mm)	3	3	3

The optimal force transmission path is obtained according to the multi-case structural topology optimization model of compromise programming. The optimization results show that the cross-

sectional shape is approximately rectangle. For the rectangle bracket, it has the advantages of convenient manufacture, reasonable stress and stable use. Most importantly, it is lighter than the solid web bracket which reduces the material consumption and lays a foundation for the subsequent gauge optimization and section shape optimization.

### 3.2. Phase II: Optimization of section shape and gauge of MEWP bracket structure under multiple working conditions

As shown in Figure 6, the control region of MEWP bracket is determined and the corresponding mesh deformation is carried out by HyperMorph. Five design variables are defined for the studied bracket, including three gauge variables and two shape variables. Moreover, the material of the three component parts in MEWP bracket (see Figure 5.) is changed from Q345 to B1500HS to improve its safety performance. The meaning, initial value, upper and lower limits of each design variable are shown in Table 5.



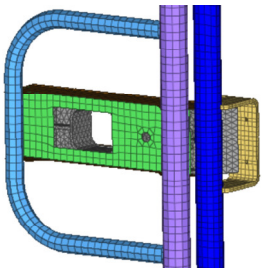
**Figure 6.** Mesh deformation of MEWP bracket.

**Table 5.** Parametric design variables of bracket.

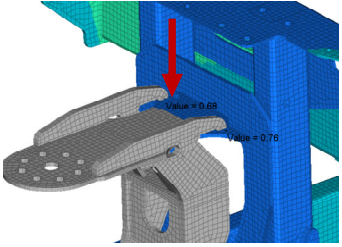
Variable number	Variable name	Initial value (mm)	Upper limit (mm)	Lower limit (mm)
1	Gauge of rectangular tube-1	3	3	1.2
2	Gauge of rectangular tube-2	3	3	1.2
3	Gauge of rectangular tube-3	3	3	1.2
4	Width of rectangular tube-1	47	51.7	42.3
5	Height of rectangular tube-1	97	106.7	87.3

For convenient description, the loading positions and magnitude of 18 forces in the five working conditions are marked as ① to ⑱ in Table 2. The displacement of the locking tab, two sensors caused by each loading force are denoted as dl<sub>tk</sub>, dl<sub>sk</sub>, dr<sub>sk</sub>, respectively (k = 1, 2, ..., 18). The Optistruct solver gets invoked for trial calculation based on the parametric model. By extracting the results from the result file, the corresponding initial values of the mass and displacement are obtained as shown in Tables 6–8.

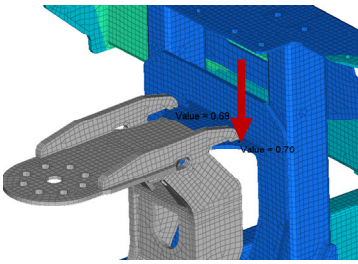
**Table 6.** Initial displacement of locking tab.

Parameter	Mass (kg)	Displacement of locking tab (mm)					
		Working condition-1		Working condition-2			Working
		①	②	③	④	⑤	⑥
Initial value	22.24	1.016	1.579	0.268	0.208	0.251	0.208
		condition-3	Working condition-4			Working	
		⑦	⑧	⑨	⑩	⑪	⑫
		0.211	0.315	0.124	0.147	0.825	0.251
		Condition-5					
		⑬	⑭	⑮	⑯	⑰	⑱
		0.053	0.082	0.201	0.189	0.677	1.599

**Table 7.** Initial displacement of left sensor.

Parameter	Mass (kg)	Displacement of left sensor (mm)					
		Working condition-1		Working condition-2			Working
		①	②	③	④	⑤	⑥
Initial value	22.24	1.904	1.891	1.935	1.892	1.892	2.290
		condition-3	Working condition-4			Working	
		⑦	⑧	⑨	⑩	⑪	⑫
		2.348	2.350	1.924	1.864	2.753	2.876
		condition-5					
		⑬	⑭	⑮	⑯	⑰	⑱
		3.042	3.036	2.855	2.666	2.568	2.630

**Table 8.** Initial displacement of right sensor.

Parameter	Mass (kg)	Displacement of right sensor (mm)					
		Working condition-1		Working condition-2		Working	
		①	②	③	④	⑤	⑥
Initial Value	22.24	1.896	1.882	1.842	1.882	1.882	2.276
		condition-3	Working condition-4		Working		
		⑦	⑧	⑨	⑩	⑪	⑫
		2.213	2.211	1.912	1.861	2.877	2.719
		condition-5					
		⑬	⑭	⑮	⑯	⑰	⑱
		2.575	2.513	2.632	2.851	3.055	3.050

The experimental design method reveals the effect of different influence factors on the response through orthogonal test. A 64 element design matrix composed of design variables and their combinations is generated by creating Latin square sampling. The upper and lower bounds of the interpolation number are set to 4. In the first round of iteration, the initial response surface is created by using the GRSM based on the internally constructed design of experiment. After the first round of iteration, a new DOE will be constructed to generate new sampling points in the area with insufficient sampling in the global design space. The response surface is updated and the optimization problem is solved on the new response surface after the DOE is executed. The optimal solution is used in the next iteration and a certain number of design points are analyzed in each iteration.

In order to minimize the weight of bracket on the basis of meeting the performance requirements of bracket, the upper limit of the displacement constraint of the locking tab is set to 2 mm, and the upper limit of the displacement of two sensors is set to the initial value. The optimization model is:

$$\text{Find: } t_i (i = 1, 2, 3), w, h$$

$$\text{Minimize: } M = \sum_{i=1}^3 m_i (i = 1, 2, 3)$$

$$\text{Subject: } 1.2\text{mm} \leq t_i \leq 3\text{mm}$$

$$42.3\text{mm} \leq w \leq 51.7\text{mm}$$

$$87.3\text{mm} \leq h \leq 106.7\text{mm}$$

$$dlt_k \leq 2\text{mm} (k = 1, 2, \dots, 18)$$

$$dls_1 \leq 1.904\text{mm} \quad dls_{10} \leq 1.864\text{mm} \quad drs_1 \leq 1.896\text{mm} \quad drs_{10} \leq 1.861\text{mm}$$

$$dls_2 \leq 1.891\text{mm} \quad dls_{11} \leq 2.753\text{mm} \quad drs_2 \leq 1.882\text{mm} \quad drs_{11} \leq 2.877\text{mm}$$

$$dls_3 \leq 1.935\text{mm} \quad dls_{12} \leq 2.876\text{mm} \quad drs_3 \leq 1.842\text{mm} \quad drs_{12} \leq 2.719\text{mm}$$

$$dls_4 \leq 1.892\text{mm} \quad dls_{13} \leq 3.042\text{mm} \quad drs_4 \leq 1.882\text{mm} \quad drs_{13} \leq 2.575\text{mm}$$

$$dls_5 \leq 1.892\text{mm} \quad dls_{14} \leq 3.036\text{mm} \quad drs_5 \leq 1.882\text{mm} \quad drs_{14} \leq 2.513\text{mm}$$

$$dls_6 \leq 2.290\text{mm} \quad dls_{15} \leq 2.855\text{mm} \quad drs_6 \leq 2.276\text{mm} \quad drs_{15} \leq 2.632\text{mm}$$

$$dls_7 \leq 2.348\text{mm} \quad dls_{16} \leq 2.666\text{mm} \quad drs_7 \leq 2.213\text{mm} \quad drs_{16} \leq 2.851\text{mm}$$

$$dls_8 \leq 2.350\text{mm} \quad dls_{17} \leq 2.568\text{mm} \quad drs_8 \leq 2.211\text{mm} \quad drs_{17} \leq 3.055\text{mm}$$

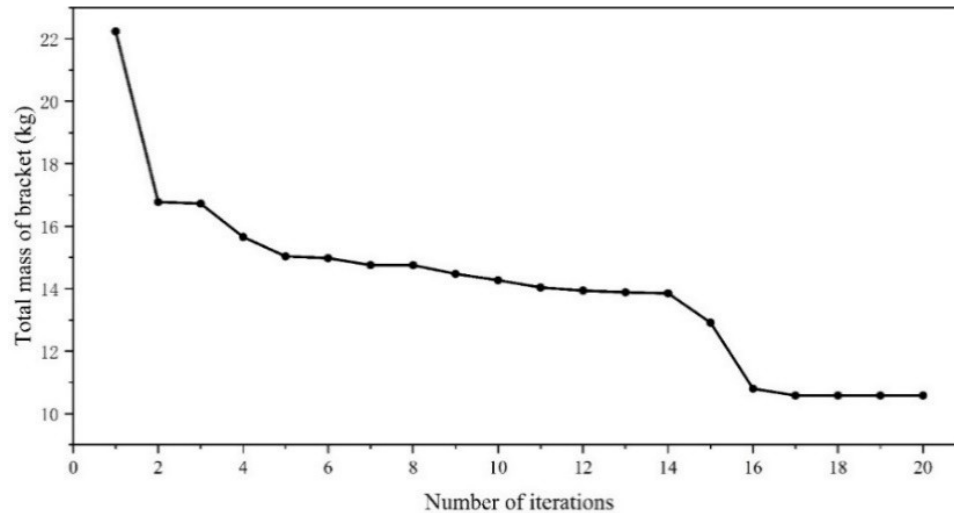
$$dls_9 \leq 1.924\text{mm} \quad dls_{18} \leq 2.630\text{mm} \quad drs_9 \leq 1.912\text{mm} \quad drs_{18} \leq 3.050\text{mm}$$

(5)

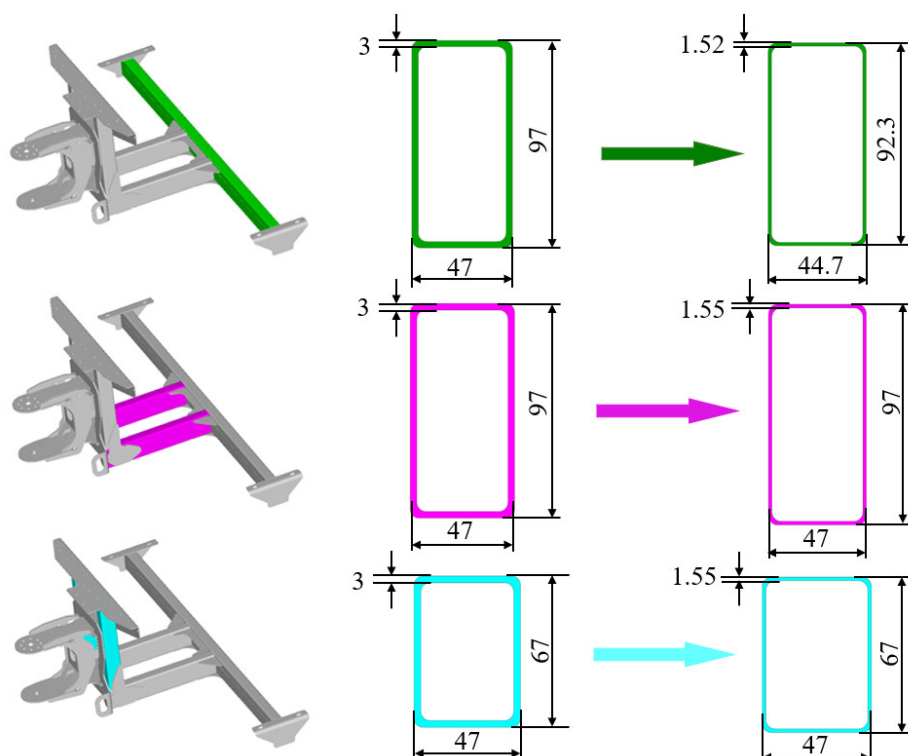
where  $t_i$  represents the gauge of the  $i$ -th rectangular tube;  $w$  is the width of rectangular tube-1;  $h$  is the height of rectangular tube-1;  $M$  is the total mass of bracket;  $m_i$  is the mass of the  $i$ -th rectangular tube.

The iterative curve of the total mass is shown in Figure 7. The weight reduction mass is 11.66 kg

and the ratio is 52.4%. Similarly, the iterative curves of gauge and cross-sectional shape are converged. The changes of cross-sectional shape and gauge of three rectangular tubes are presented in Figure 8. After optimization, the gauge of three rectangular tubes are 1.52, 1.55 and 1.55 mm, respectively. Moreover, the width and height of rectangular tube-1 is about 44.7 and 92.3 mm, respectively.



**Figure 7.** Iterative curve of total mass.



**Figure 8.** Cross-sectional shape and gauge before and after optimization.



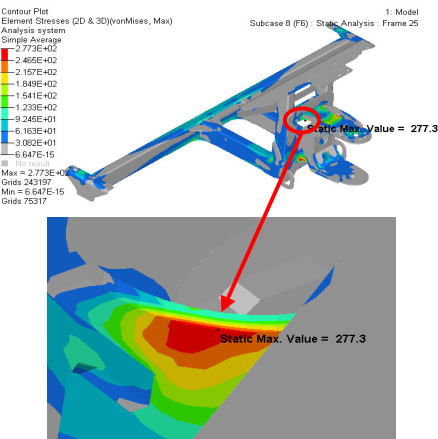
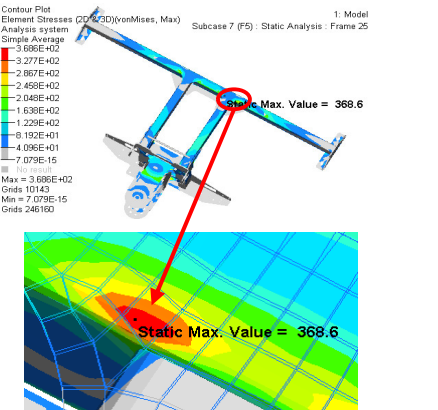
### 3.3. Comparison and discussion

The optimized results of phase I and phase II under the most extreme working condition (i.e., working condition 3) are listed in Table 9. It can be seen from Table 9 that the maximum stress of the MEWP bracket after phase I and phase II are 277.3 and 368.6 MPa, respectively. However, the ultimate stress of B1500HS (1500 MPa) is much larger than the Q460 (630 MPa), the safety factor of the MEWP after phase II has a great larger than it after phase I. Note that the safety factor can be defined by Eq (6).

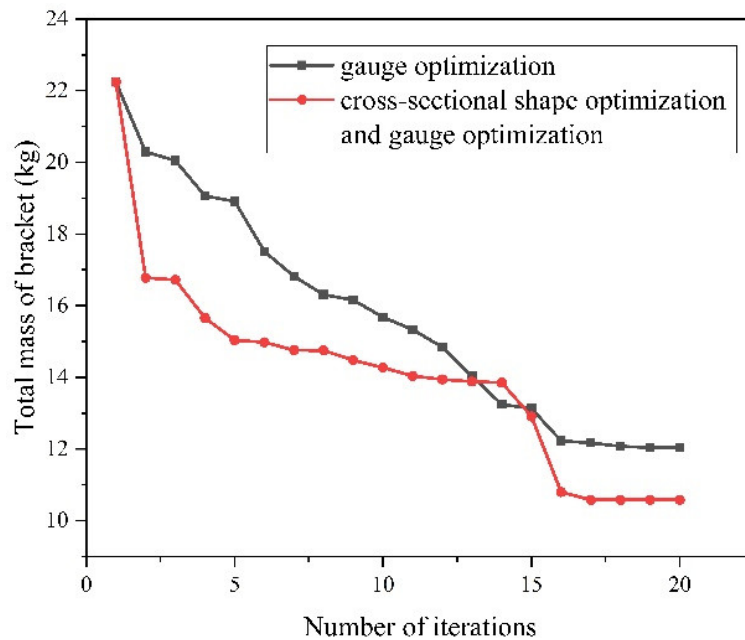
$$\text{Safety factor} = \frac{\text{Ultimate stress}}{\text{Maximum stress}} \quad (6)$$

In order to prove the effectiveness of the multi-level optimization method, this paper carries out design optimization under single gauge optimization. After optimization, the weight of bracket is also reduced. Specifically, the weight reduction mass is 10.39 kg and the ratio is 46.7%. The gauge of the three rectangular tubes are 1.57, 1.58 and 1.58 mm respectively.

**Table 9.** Optimized results of phase I and phase II under working condition 3.

Phase	Von mises stress (MPa)	Material	Maximum stress (MPa)	Safety factor
Phase I		Q460	277.3	2.27
Phase II		B1500HS	368.6	4.06

As shown in Figure 9, the lightweight iteration curves under two optimization methods are iteratively convergent. The weight reduction effect under multi-level optimization is more obvious than that under single gauge optimization. The weight reduction mass is 11.66 kg and the ratio is 52.4%. Compared with the single thickness optimization, the weight is further reduced by 1.27 kg under multi-level optimization.



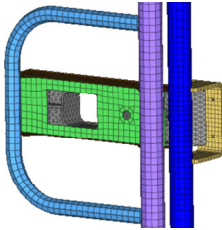
**Figure 9.** Comparison of iterative curves of lightweight effect.

The changes of design variables and optimization objectives are shown in Tables 10–13. It can be seen that the gauge of three rectangular tubes and the section size of rectangular tube-1 under multi-level optimization are smaller than those under single thickness optimization.

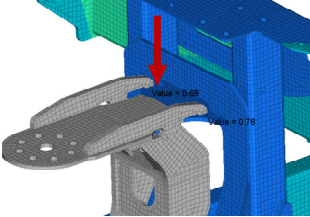
**Table 10.** Comparison of optimization results under two means of optimization.

Means of optimization	Mass (kg)	Weight reduction ratio(%)	Gauge of rectangular tube-1	Gauge of rectangular tube-2	Gauge of rectangular tube-3	Width of rectangular tube-1	Height of rectangular tube-1
Initial design	22.24		3.00 mm	3.00 mm	3.00 mm	47.0 mm	97.0 mm
Gauge optimization	11.85	46.7	1.57 mm	1.58 mm	1.58 mm	47.0 mm	97.0 mm
Cross-sectional shape and gauge optimization	10.58	52.4	1.52 mm	1.55 mm	1.55 mm	44.7 mm	92.3 mm

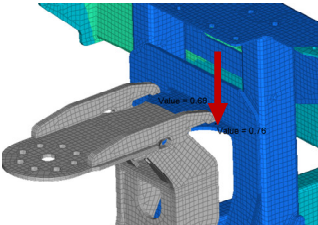
**Table 11.** Comparison of locking tab displacement under two means of optimization.

Parameter	Displacement of locking tab (mm)					
	Working condition-1		Working condition-2			Working
	①	②	③	④	⑤	⑥
Initial value	1.016	1.579	0.268	0.208	0.251	0.208
Cross-sectional shape and gauge optimization	0.813	1.324	0.115	0.127	0.149	0.127
Gauge optimization	0.908	1.505	0.185	0.177	0.207	0.177
	condition-3		Working condition-4			Working
	⑦	⑧	⑨	⑩	⑪	
	0.211	0.315	0.124	0.147	0.825	
	0.207	0.283	0.122	0.124	0.728	
	0.177	0.312	0.089	0.112	0.808	
condition-5						
⑫	⑬	⑭	⑮	⑯	⑰	⑱
0.251	0.053	0.082	0.201	0.189	0.677	1.599
0.137	0.027	0.041	0.160	0.159	0.563	1.521
0.248	0.037	0.070	0.195	0.189	0.509	1.432

**Table 12.** Comparison of left sensor displacement under two means of optimization.

Parameter	Displacement of left sensor (mm)					
	Working condition-1		Working condition-2			Working
	①	②	③	④	⑤	⑥
Initial value	1.904	1.891	1.935	1.892	1.892	2.290
Optimization of cross-sectional shape and gauge	1.796	1.818	1.853	1.862	1.848	2.261
Gauge optimization	1.902	1.887	1.935	1.887	1.887	2.273
	condition-3		Working condition-4			Working
	⑦	⑧	⑨	⑩	⑪	
	2.348	2.350	1.924	1.864	2.753	
	2.314	2.347	1.890	1.830	2.736	
	2.327	2.318	1.923	1.856	2.710	
condition-5						
⑫	⑬	⑭	⑮	⑯	⑰	⑱
2.876	3.042	3.036	2.855	2.666	2.568	2.630
2.825	2.548	2.472	2.592	2.821	2.941	2.972
2.873	2.563	2.491	2.621	2.844	3.031	3.024

**Table 13.** Comparison of right sensor displacement under two means of optimization.

Parameter	Displacement of right sensor (mm)					Working condition-5
	Working condition-1		Working condition-2		Working condition-3	
	①	②	③	④	⑤	⑥
Initial value	1.896	1.882	1.842	1.882	1.882	2.276
Optimization of cross-sectional shape and gauge	1.785	1.807	1.758	1.851	1.838	2.245
Gauge optimization	1.890	1.876	1.831	1.876	1.876	2.274
						
Working condition-5						
⑫	⑬	⑭	⑮	⑯	⑰	⑱
2.719	2.575	2.513	2.632	2.851	3.055	3.050
2.716	2.548	2.472	2.592	2.821	2.941	2.972
2.711	2.563	2.491	2.621	2.844	3.031	3.024

It can be found that the displacement of locking tab and sensors under multi-level optimization is further reduced compared with single gauge optimization, which means the stiffness has been further improved. According to the above results of optimization, the geometric model of MEWP bracket is reconstructed. The developed physical prototype is shown in Figure 10.

**Figure 10.** Physical drawing of prototype.

#### 4. Conclusions

This paper takes the MEWP as the research object and carries out the structural lightweight design of bracket based on the multi-level optimization method. The optimized structure reduces the material

consumption and improves the performance and stability of MEWP.

Firstly, the multi-case topology optimization model of MEWP bracket is constructed based on the compromise programming method and SIMP topology optimization theory. The rectangular cross section of MEWP bracket is obtained. Secondly, the optimal cross-sectional shape and gauge of the MEWP bracket are obtained by using multi-level optimization method. The results show that the weight reduction mass of bracket is about 11.66 kg and the ratio is 52.4%. The mass of bracket is further reduced by 1.27 kg compared with the single gauge optimization, which proves the effectiveness of the multi-level optimization method. Finally, the physical prototype is developed according to the optimization results.

## Acknowledgments

This work is supported from the Open Fund Program of the State Key Laboratory of Intelligent Manufacturing of Advanced Construction Machinery (No. Kfkt202002).

## Conflict of interest

The raw/processed test data required to reproduce these findings cannot be shared at this time due to both legal reasons and time limitations.

## References

1. Z. Wang, X. Liu, Lightweight optimization design of arm frame for aerial work platform based on NSGA-II algorithm, *IOP Conf. Ser.: Mater. Sci. Eng.*, **733** (2020), 012037. <https://doi.org/10.1088/1757-899X/733/1/012037>
2. G. Sun, H. Zhang, J. Fang, G. Li, Q. Li, Multi-objective and multi-case reliability-based design optimization for tailor rolled blank (TRB) structures, *Struct. Multidiscip. Optim.*, **55** (2017), 1899–1916. <https://doi.org/10.1007/s00158-016-1592-1>
3. L. Duan, H. Jiang, A. Cheng, H. Xue, G. Geng, Multi-objective reliability-based design optimization for the VRB-VCS FLB under front-impact collision, *Struct. Multidiscip. Optim.*, **59** (2019), 1835–1851. <https://doi.org/10.1007/s00158-018-2142-9>
4. N. Qiu, Y. Gao, J. Fang, G. Sun, N. H. Kim, Topological design of multi-cell hexagonal tubes under axial and lateral loading cases using a modified particle swarm algorithm, *Appl. Math. Modell.*, **53** (2018), 567–583. <https://doi.org/10.1016/j.apm.2017.08.017>
5. A. Y. Ismail, G. Na, B. Koo, Topology and response surface optimization of a bicycle crank arm with multiple load cases, *Appl. Sci.*, **10** (2020), 2201. <https://doi.org/10.3390/app10062201>
6. Y. X. Du, J. R. Hu, Z. F. Fang, Q. H. Tian, Topology optimization for work flat of tower-belt under multi-loading cases, *Appl. Mech. Mater.*, **197** (2012), 614–618. <https://doi.org/10.4028/www.scientific.net/AMM.197.614>
7. Y. Wang, H. T. Zhu, L. Xu, J. P. Ji, X. L. Dai, Study on optimization of engine accessory bracket based on optistruct, *Adv. Mater. Res.*, **421** (2012), 308–311. <https://doi.org/10.4028/www.scientific.net/AMR.421.308>

8. C. Zhuang, Z. Xiong, H. Ding, A level set method for topology optimization of heat conduction problem under multiple load cases, *Comput. Methods Appl. Mech. Eng.*, **196** (2007), 1074–1084. <https://doi.org/10.1016/j.cma.2006.08.005>
9. L. Duan, N. Xiao, Z. Hu, G. Li, A. Cheng, An efficient lightweight design strategy for body-in-white based on implicit parameterization technique, *Struct. Multidiscip. Optim.*, **55** (2017), 1927–1943. <https://doi.org/10.1007/s00158-016-1621-0>
10. B. Mi, S. Cheng, Y. Luo, H. Fan, A new many-objective aerodynamic optimization method for symmetrical elliptic airfoils by PSO and direct-manipulation-based parametric mesh deformation, *Aerosp. Sci. Technol.*, **120** (2022), 107296. <https://doi.org/10.1016/j.ast.2021.107296>
11. W. Zhang, S. Feng, Combined parameterization of material distribution and surface mesh for stiffener layout optimization of complex surfaces, *Struct. Multidiscip. Optim.*, **65** (2022), 103. <https://doi.org/10.1007/s00158-022-03191-3>
12. C. Zhang, S. Yang, Q. Zhang, G. Zhao, P. Lu, W. Sun, Automatic optimization design of a feeder extrusion die with response surface methodology and mesh deformation technique, *Int. J. Adv. Manuf. Technol.*, **91** (2017), 3181–3193. <https://doi.org/10.1007/s00170-017-0018-6>
13. D. Wang, R. Jiang, Y. Wu, A hybrid method of modified NSGA-II and TOPSIS for lightweight design of parameterized passenger car sub-frame, *J. Mech. Sci. Technol.*, **30** (2016), 4909–4917. <https://doi.org/10.1007/s12206-016-1010-z>
14. A. Nazemian, P. Ghadimi, Shape optimisation of trimaran ship hull using CFD-based simulation and adjoint solver, *Ships Offshore Struct.*, **17** (2022), 359–373. <https://doi.org/10.1080/17445302.2020.1827807>
15. W. Hou, C. Shan, P. Hu, H. Zhang, Multilevel optimisation method for vehicle body in conceptual design, *Int. J. Veh. Des.*, **73** (2017), 157–178. <https://doi.org/10.1504/IJVD.2017.082589>
16. I. Gandikota, M. Rais-Rohani, M. Kiani, S. DorMohammadi, Multilevel design optimisation of a vehicle-dummy model under crash, vibration and injury criteria, *Int. J. Veh. Des.*, **70** (2015), 45–68. <https://doi.org/10.1504/IJVD.2016.073703>
17. X. Liu, W. He, F. Wei, Design of high altitude propeller using multilevel optimization, *Int. J. Comput. Methods*, **17** (2020), 1950004. <https://doi.org/10.1142/S021987621950004X>
18. M. P. Bendsøe, N. Kikuchi, Generating optimal topologies in structural design using a homogenization method, *Comput. Methods Appl. Mech. Eng.*, **71** (1988), 197–224. [https://doi.org/10.1016/0045-7825\(88\)90086-2](https://doi.org/10.1016/0045-7825(88)90086-2)



AIMS Press

©2022 the Author(s), licensee AIMS Press. This is an open access article distributed under the terms of the Creative Commons Attribution License (<http://creativecommons.org/licenses/by/4.0>)